

RJMMC-BASED TRACKING OF VESICLES IN FLUORESCENCE TIME-LAPSE MICROSCOPY

David Nam¹, Kenton Arkill², Richard Eales¹, Lorna Hodgson², Paul Verkade^{2,3,4,†}, and Alin Achim^{1,†}

¹Visual Information Laboratory, ²School of Biochemistry, ³Wolfson Bioimaging Facility,

⁴School of Physiology and Pharmacology. University of Bristol, Bristol, UK.

ABSTRACT

Vesicles are a key component for the transport of materials throughout the cell. To manually analyze the behaviors of vesicles in fluorescence time-lapse microscopy images would be almost impossible. This is also true for the identification of key events, such as merging and splitting. In order to automate and increase the reliability of this processes we introduce a Reversible Jump Markov chain Monte Carlo method for tracking vesicles and identifying merging/splitting events, based on object interactions. We evaluate our method on a series of synthetic videos with varying degrees of noise. We show that our method compares well with other state-of-the-art techniques and well-known microscopy tracking tools. The robustness of our method is also demonstrated on real microscopy videos.

Index Terms— Light microscopy, biomedical imaging, MCMC, merging, splitting

1. INTRODUCTION

Specific molecules can be located in cells using fluorescence microscopy. Fluorescent molecules absorb light at a particular wavelength and emit light, at a longer wavelength. Laser scanning confocal microscopy is a modality used for viewing fluorescence within cells [1]. Many individual objects have to be tracked to obtain robust and sound conclusions. However, tracking subcellular particles is challenging. Problems are due to the small sizes of these particles as well as their behavior. In addition, one has to cope with large numbers of particles, making manual tracking infeasible, as well as a relatively low signal-to-noise ratio (SNR).

Due to the limited spatial resolution of the microscope, a vesicle is displayed as a dot. The small size of vesicles means that not many fluorescent molecules may be attached to them. The resulting low contrast of each vesicle makes its identification against the cellular autofluorescent—the natural emission of light by biological structures—background challenging. Furthermore their complex motion, which includes sudden changes in speed and direction, make tracking particularly challenging. Vesicles may also move out of the

focal plane during observation; this leads to a change in appearance. Additionally, the large number of vesicles in the image sequences rules out algorithms that are only applicable to one object or few objects.

Conventional approaches to tracking in molecular cell biology typically consist of two steps, detection in each image frame and correspondence, using the nearest neighbors. This approach to object tracking is only applicable to videos which show a few clearly distinguishable objects against a uniform background. They are however unable to cope with cases containing poor imaging conditions. To obtain better temporal associations, in videos with low SNR's, high object densities and complex motion, it is necessary to make better use of temporal information and prior knowledge.

In [2] a particle tracking method for clathrin mediated endocytosis analysis was proposed. Fluorescence images were acquired using total internal reflection microscopy and the multiple hypothesis tracking (MHT) framework was extended by considering multiple observation candidates and more types of trajectory candidates. MHT maintains a tree of hypotheses for all possible associations, which results in an exponentially growing number of hypotheses. Sequential Monte Carlo (SMC) methods are typically applied in cases of nonlinearity and nonGaussian statistics, in particular particle filtering (PF). In [3] a mixture of PFs was used for tracking microtubule growth in fluorescence confocal microscopy. PFs are again employed in [3], for tracking virus particles in time-lapse fluorescence microscopy. Detailed analysis was done, comparing a mixture of PFs, independent PFs, and other deterministic approaches. In their analysis [3] demonstrated the superior performance of independent PFs, for tracking a large number of targets.

Markov Chain Monte Carlo (MCMC) based tracking methods have an advantage over conventional PFs [4]. They are more effective in high-dimensional spaces and do not have the same degeneracy problems faced by PFs [5]. [6] explains that running one individual PF for each target is not a viable option and that it does not address the complex interactions between targets and leads to frequent tracking failures. They also demonstrate the superior performance of their MCMC based tracker against a standard PF and independent PFs.

In this paper we present a MCMC based tracking algo-

[†] shared last author

rithm, with reversible jumps (RJMCMC), to tracking a large number of vesicles, in fluorescence confocal microscopy time-lapse images. We introduce methods to distinguish between vesicle birth from splitting and death from merging. Theoretical preliminaries are discussed in Section. 2. Details of our RJMCMC tracking algorithm are presented in Section. 3. Experimental results are shown in Section. 4 and we conclude in Section. 5.

2. BAYESIAN FOUNDATIONS FOR OBJECT TRACKING

Under the commonly made assumption that target motion is Markovian, the Bayes filter offers a formulation to tackle the problem of tracking multiple objects. The recursive relation is often intractable since complex high dimensional integrals must be solved. The Kalman filter provides an analytical solution if the dynamical and measurement models are linear and Gaussian. However this is not always the case, and an analytical solution cannot always be obtained. In this case Monte Carlo methods are commonly used to approximate the solution.

Given a time-lapse video, with objects to be tracked, we assume that an object is represented by a state vector $\{\mathbf{x}_t : t = 1, 2, \dots\}$ and a noisy measurement $\{\mathbf{z}_t : t = 1, 2, \dots\}$, where $\mathbf{x}_{1:t} \triangleq \{\mathbf{x}_1, \dots, \mathbf{x}_t\}$ and $\mathbf{z}_{1:t} \triangleq \{\mathbf{z}_1, \dots, \mathbf{z}_t\}$ represent the state and observations up to time t , respectively. Here the state \mathbf{x} represents an objects coordinates. At each time step the posterior probability density function (PDF) $p(\mathbf{x}_t | \mathbf{z}_{1:t})$ is computed by first obtaining the prior PDF $p(\mathbf{x}_t | \mathbf{z}_{1:t-1})$ and then updating with the new measurement \mathbf{z}_t using Bayes' theorem:

$$p(\mathbf{x}_t | \mathbf{z}_{1:t-1}) = \int p(\mathbf{x}_t | \mathbf{x}_{t-1}) p(\mathbf{x}_{t-1} | \mathbf{z}_{1:t-1}) d\mathbf{x}_{t-1}. \quad (1)$$

$$p(\mathbf{x}_t | \mathbf{z}_{1:t}) \propto p(\mathbf{z}_t | \mathbf{x}_t) p(\mathbf{x}_t | \mathbf{z}_{1:t-1}). \quad (2)$$

In (1) and (2), $p(\mathbf{x}_t | \mathbf{x}_{t-1})$ is commonly called the motion or dynamical model and $p(\mathbf{z}_t | \mathbf{x}_t)$ the measurement or observation model. From the posterior distribution (2), we are able to estimate \mathbf{x}_t given \mathbf{z}_t . PF based methods approximate (2), by using N particles that are weighted based on importance. The weighted particles are then propagated in time. Below we describe our MCMC approach to estimating (2) and \mathbf{x}_t .

3. TRACKING A VARIABLE NUMBER OF VESICLES USING RJMCMC

Due to the limitations of importance sampling in high dimensional state spaces, researchers have applied MCMC methods to tracking problems. One advantage is that MCMC methods are flexible and can sample only a part of the state conditional

upon the rest, thus facilitating efficient samples. One main advantage with MCMC methods is its ability to cope with high dimensional state spaces. All MCMC methods work by defining a Markov Chain over the space of configurations \mathbf{x} , such that the stationary distribution $\pi(\mathbf{x})$ of the chain is used to approximate the posterior $p(\mathbf{x}_t | \mathbf{z}_{1:t})$ over the set \mathbf{x} given the measurements \mathbf{z} . If we denote the total number of states, (at frame t) as n , then the object specific state is \mathbf{x}_{kt} , (where $k \in \mathbb{Z} : k = 1, \dots, n$).

The Metropolis-Hastings (MH) algorithm [7] is a frequently used method for generating samples from $\pi(\mathbf{x})$. It is an iterative method where each sample is generated based on an acceptance probability. If there are N samples, $\pi(\mathbf{x})$ is approximated at time t as $\{\mathbf{x}_t^{(i)}\}_{i=1}^N \approx p(\mathbf{x}_t | \mathbf{z}_t)$. In order to generate the acceptance probabilities new samples are drawn, based on a proposal density $Q(\mathbf{x}'_{kt}; \mathbf{x}_{kt})$, where \mathbf{x}'_{kt} is a proposal state. Here we perturb the target state by setting the proposal density to a normal distribution (standard deviation 1) around \mathbf{x}_{kt}^i [6].

3.1. Observation and motion models

For our observation model we use a Gaussian function located at \mathbf{x} as $g(\mathbf{x})$ to estimate vesicles. Gaussian fitting for tracking in fluorescence microscopy applications has been demonstrated to be robust, [8], [3]. In our applications we fix the standard deviation of the Gaussian to match the size of a vesicle and we also normalize the intensities. Although these parameters can be included in the state vector, we found that our approach gave good results for our applications. Therefore given an observation \mathbf{z} we define our measurement model as:

$$p(\mathbf{z} | \mathbf{x}) \propto \exp(-D(\mathbf{z}, g(\mathbf{x}))^2). \quad (3)$$

Where D is the Euclidean distance (in a window 3 times the radius of a vesicle).

Typically, vesicles seem to exhibit a random motion. For our motion model we assume the vesicles follow a Gaussian Random walk, with standard deviation $\sigma_{\mathbf{x}}$.

3.2. Object interactions

It is sometimes possible for trackers to be attracted to the same objects, when multiple objects are close by. This is usually undesirable and will result in tracking failures. [6] proposed to model object interactions using a pairwise Markov Random Field (MRF), created at each step (V, E) . Object interactions are incorporated into the motion model, such that:

$$p(\mathbf{x}_t | \mathbf{x}_{t-1}) \propto \prod_j p(\mathbf{x}_{jt}, \mathbf{x}_{j(t-1)}) \prod_{j_1, j_2 \in E} \psi(\mathbf{x}_{j_1 t}, \mathbf{x}_{j_2 t}). \quad (4)$$

Where $\psi(\mathbf{x}_{j_1 t}, \mathbf{x}_{j_2 t})$ is a pairwise interaction potential; given my means of a Gibbs distribution such that, $\psi(\mathbf{x}_{j_1 t}, \mathbf{x}_{j_2 t}) \propto$

$\exp(-d_{(j_1, j_2)})$ and $j_1 \neq j_2$. For split/merge moves we want objects that are juxtaposed to give a higher acceptance ratio, therefore we propose using $\psi_{s/m}(\mathbf{x}_{j_1 t}, \mathbf{x}_{j_2 t}) \propto \exp(d_{(j_1, j_2)} - 1)$, for these moves. Here $d_{(j_1, j_2)}$ is a penalty function from allowing two states to be too close together. We define $d_{(j_1, j_2)}$ to be the Dice's coefficient between two circles (radius=vesicle radius) located at the positions of objects j_1 and j_2 . Moreover, the interaction term can be factored out of the motion model and be treated as an additional factor.

3.3. Reversible-Jumps

In the RJMCMC method [9], the MH algorithm is extended to handle trans-dimensional moves, therefore increasing or decreasing the number of objects being tracked. When there is a varying number of objects to be tracked each sample will include a set of identifiers k_t , which $p(k_t, \mathbf{x}_t | \mathbf{z}_t) \propto \{k_t^{(i)}, \mathbf{x}_t^{(i)}\}_{i=1}^N$ [6]. The algorithm selects a move—a move that can alter the dimensionality is referred to as a jump—and then proposes a new state (k'_t, \mathbf{x}'_t) , based on the proposal density $Q_m(k'_t, \mathbf{x}'_{kt}; k_t, \mathbf{x}_{kt})$ from the move type selected. Every jump should have a corresponding reverse jump; here we denote the reverse proposal density as $Q_{m'}(k_t, \mathbf{x}_{kt}; k'_t, \mathbf{x}'_{kt})$, where m' is the reverse jump to move m .

For our application of tracking vesicles, we propose the following sets of moves m : birth/death, split/merge, and update. Being able to distinguish split/merge events from a birth/death events (respectively), is a useful task in cellular biology. Identifying occasions of vesicles merging can indicate the transfer of cargo. Automatically highlighting these rare events will allow biologists to better understand complex protein mechanisms that happen during vesicle merging. Here a birth scenario is usually associated with an object moving into the microscope's field of view or coming into the focal plane and likewise for object death. A split however is the creation of a new vesicle from an existing one; the opposite for merging. The probabilities of selecting a birth, death, split, merge, or update move are: p_b, p_d, p_s, p_m, p_u , respectively. For each move, in order to estimate $p(k_t, \mathbf{x}_t | \mathbf{z}_t)$ an acceptance ratio must be calculated, for each sample. The acceptance ratio is as follows:

$$a = \frac{p(k'_t, \mathbf{x}'_{kt} | \mathbf{z}_t) p_{m'} Q_{m'}(k_t, \mathbf{x}_{kt}; k'_t, \mathbf{x}'_{kt})}{p(k_t, \mathbf{x}_{kt} | \mathbf{z}_t) p_m Q_m(k'_t, \mathbf{x}'_{kt}; k_t, \mathbf{x}_{kt})}. \quad (5)$$

Vesicle detection

The subsequent jump moves are facilitated by our vesicle detection. Given a frame at time t as I_t , our vesicle detection scheme is as follows: 1) obtain an image mask by thresholding I_t , by the 95th percentile, of all nonzero pixels. 2) Given a Gaussian smoothed (with a standard deviation the diameter of a vesicle) version of I_t , apply the mask to obtain I_{tm} . 3)

The set of detected target identifiers k_d , is obtained by locating the regional maxima of I_{tm} . With a method to detect new vesicles we can define our jump proposals as follows:

Birth

In the birth step we propose adding a detected object O_b to the identifier set k_t , by selecting an object with probability $Q_b = \frac{1}{|k_d \setminus k_t|}$. Where $(k_d \setminus k_t) \notin k_t$, is the set of objects that have been detected but are not a part of k_t . Correspondences are made by the nearest neighbor method. If no new object is detected then $Q_b = 0$.

Death

Again we facilitate out death move using our object detector. Here we use $(k_t \cap k_d)$, as the set of objects k_t that are corresponding with more than one object in k_d . An object O_d is selected $Q_d = \frac{1}{|k_t \cap k_d|}$. If all tracked states are accounted for, otherwise $Q_d = 0$.

Split/Merge

Since splitting and merging are, in principle, specialized cases of births and deaths, we used the same proposal densities as for births and deaths, respectively. The split move is defined similarly to the birth move, but with the assumption that the birth happens juxtaposed to another vesicle and similarly for deaths and merging.

Acceptance ratios

The corresponding acceptance ratios for the different move types can be obtained from (2) and (5):

$$a_b = p(\mathbf{z}_t | \mathbf{x}_b) \frac{p(k'_t, \mathbf{x}'_{kt} | \mathbf{z}_{1:t-1}) \prod_{j_1 \in E} \psi(\mathbf{x}_b, \mathbf{x}_{j_1 t})}{p(k_t, \mathbf{x}_{kt} | \mathbf{z}_{1:t-1})} \times \frac{p_d |k_d \setminus k_t|}{p_b |k'_t \cap k_d|}, \quad (6)$$

$$a_d = \frac{1}{p(\mathbf{z}_t | \mathbf{x}_d)} \frac{p(k'_t, \mathbf{x}'_{kt} | \mathbf{z}_{1:t-1}) \prod_{j_1 \in E} \psi(\mathbf{x}_d, \mathbf{x}_{j_1 t})}{p(k_t, \mathbf{x}_{kt} | \mathbf{z}_{1:t-1})} \times \frac{p_b |k_t \cap k_d|}{p_d |k_d \setminus k'_t|}, \quad (7)$$

$$a_s = p(\mathbf{z}_t | \mathbf{x}_s) \frac{p(k'_t, \mathbf{x}'_{kt} | \mathbf{z}_{1:t-1}) \prod_{j_1 \in E} \psi_{s/m}(\mathbf{x}_s, \mathbf{x}_{j_1 t})}{p(k_t, \mathbf{x}_{kt} | \mathbf{z}_{1:t-1})} \times \frac{p_m |k_d \setminus k_t|}{p_s |k'_t \cap k_d|}, \quad (8)$$

$$a_m = p(\mathbf{z}_t | \mathbf{x}_m) \frac{p(k'_t, \mathbf{x}'_{kt} | \mathbf{z}_{1:t-1}) \prod_{j_1 \in E} \psi_{s/m}(\mathbf{x}_m, \mathbf{x}_{j_1 t})}{p(k_t, \mathbf{x}_{kt} | \mathbf{z}_{1:t-1})} \times \frac{p_b |k_t \cap k_d|}{p_d |k_d \setminus k'_t|}. \quad (9)$$

Algorithm 1: RJMCMC vesicle tracker

 Generate samples $(k_t^i, \mathbf{x}_t^i)_{i=1}^n$.

for $k = 1, \dots, n$ **do**

 • Initialize sampler where target $(k_{t-1}, \mathbf{x}_{t-1})$ is updated according to the motion model, and used as the initial sample in the Markov Chain.

for $i = 1, \dots, (N + B)$ **do**

 /* B is the burn-in iterations, where samples are not stored during this period. */

 • Select a move type m , where

 $p_u = (1 - (p_b + p_d + p_s + p_m))$.

 • Obtain the new (k'_t, \mathbf{x}'_t) , based on the move selected.

• Calculate the acceptance ratio

 $a = \min(1, a)$, based on the move type from: ((6),(7),(8),(9),(10)).

 • Accept the proposed move with probability a i.e. $(k_t^i, \mathbf{x}_t^i) = (k'_t, \mathbf{x}'_t)$; otherwise set as previous sample.

 • If a move type that increases dimensionality is selected: $(k_t, \mathbf{x}_{kt}) \cup (O_b, \mathbf{x}_b/\mathbf{x}_s)$.

 • If a move type that decreases dimensionality is selected: $(k_t, \mathbf{x}_{kt}) \setminus (O_d, \mathbf{x}_d/\mathbf{x}_m)$.

end
end

$$a_u = \frac{p(\mathbf{z}_t | k'_t, \mathbf{x}'_{kt}) p(k'_t, \mathbf{x}'_{kt} | \mathbf{z}_{1:t-1}) Q_{m'}(k_t, \mathbf{x}_{kt}; k'_t, \mathbf{x}'_{kt})}{p(\mathbf{z}_t | k_t, \mathbf{x}_{kt}) p(k_t, \mathbf{x}_{kt} | \mathbf{z}_{1:t-1}) Q_m(k'_t, \mathbf{x}'_{kt}; k_t, \mathbf{x}_{kt})}. \quad (10)$$

Where $j_1 \neq O_d$ in (7) and (9). The interaction terms for the proposed merge and split moves discourage those moves to be taken if the potential object is not in close proximity to another target. By only considering the state of one object per iteration, most factors in the above acceptance ratios cancel and only one likelihood calculation needs to be done per iteration.

3.4. Managing short lived detections

Our method of adding or removing from the number of objects being tracked is facilitated by a vesicle detector. However, during image acquisitions there may be many spurious detections. These are attributed to autofluorescence or vesicles that only temporarily enter the field of view. Although detected, there is little need in tracking these spurious objects. [3] encountered a similar problem; when tracking virus particles. We adopt a similar approach, where we pass our detected and tracked objects through a buffer, before actually tracking them. Given the set of objects being tracked \mathbf{x}_{kt} , upon detection at time t_d they are initially placed in a buffer, \mathbf{x}_{kt}^B . Once $(t - t_d) > t_{thresh}$, the object is taken out of the

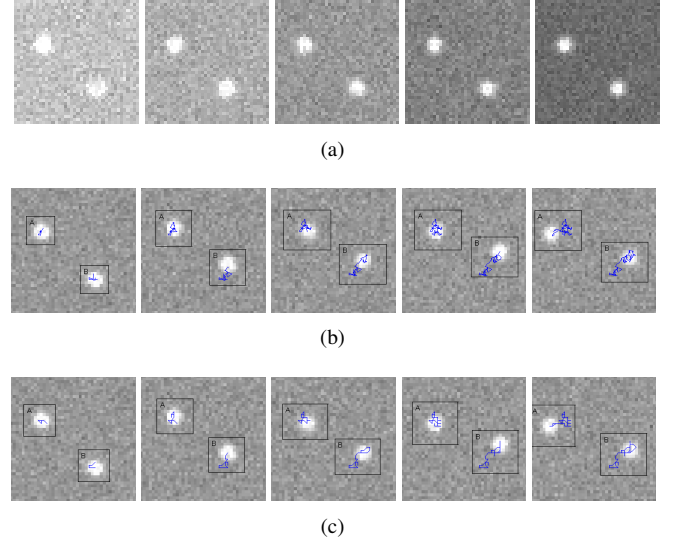


Fig. 1. Examples of varying SNRs used and sequence of tracks from the proposed methods and the ground truth.

buffer and its track is recorded; however if it is removed before the threshold its track will be purged from the record of tracks.

4. EXPERIMENTAL RESULTS

We test our method using synthetic and real microscopy videos. We set σ_x to 0.3, p_b and $p_d = 0.08$, p_s and $p_m = 0.05$, and $t_{thresh} = 5$. The RJMCMC method is set to 40 iterations with a 20% burn-in. We also scale our interaction terms by 10, for emphasis. Our simulated videos (512×512) contained 40 vesicles, modeled as a Gaussian with a standard deviation of 1.5 pixels. They were also varied in intensity and exhibited a random motion. Vesicle birth, death, splitting, and merging was also simulated (where vesicles could also move outside the boundary). We also added Poisson noise to our simulations, with 5 equally spaced SNRs, (SNR=1.91-7.68). Here SNR is defined as in [8]. We denote our images as Seq_{1-5} , where Seq_1 has the lowest SNR. Examples of Seq_{1-5} are shown in Fig. 1 (a) for a section of our test videos, from a single frame. We also show the tracks—in blue—for a section of Seq_3 , (for frames: 10, 30, 45, 60 and 75) in Fig. 1 (b) and the corresponding ground truth tracks in Fig. 1 (c).

We use two metrics to compare our results, firstly the root mean square error (RMSE). In the RMSE we use the Euclidean distance between our tracked vesicles and the ground truth, for corresponding vesicles. We also calculate the percentage accuracy, which is the ratio of correct tracks to the total number of tracks. A track is said to be correct if it is within 3 pixels of its corresponding ground truth track. These results are shown in Table 1, we also show results from a well established microscopy object tracker, u-track [10]. Our results

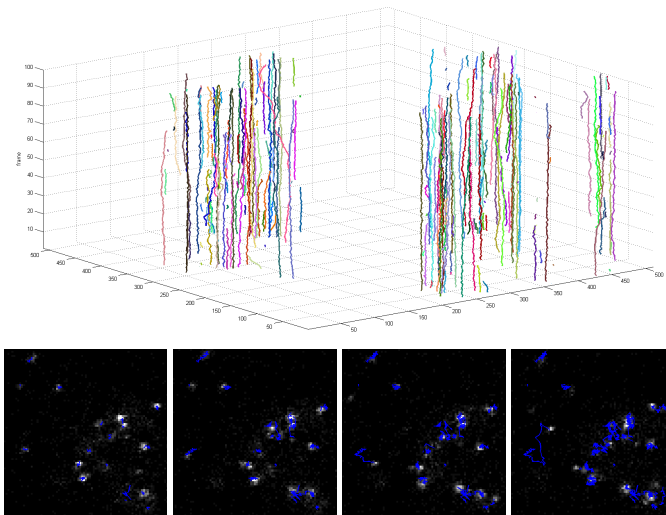


Fig. 2. Vesicle pathways for real microscopy video (top). Vesicle tracks (blue) at different time frames (bottom row).

Seq_{1-5}	Seq_1	Seq_2	Seq_3	Seq_4	Seq_5
RMSE	1.23	1.05	0.85	0.93	0.84
Accuracy(%)	95.7	96.1	98.3	96.9	98.2
RMSE [10]	1.75	1.75	1.74	1.73	1.72
Accuracy(%) [10]	93.9	93.9	93.8	93.8	93.9

Table 1. Comparison of proposed method and u-track against ground truth, with varying SNRs.

also compare favorably, on similar tests, with other state-of-the-art tracking techniques [8].

To evaluate our merging and splitting moves we calculated for RMSE (but also including time) for the detection of both events. The merging tests were one on a 200×200 video containing 50 vesicles with $SNR = 4.1$. All merges were detected, with an RMSE of 3.5. Splitting was done on a similar video, but with 10 vesicles. All splits were observed but with a RMSE of 12.7. Improvements to these moves can be made by changing the observation model (to reduce false positives); this will be the focus of future work. We also demonstrate our results on real microscopy videos (transferrin bound to Alexa Fluor 488), with dimensions $((512 \times 512) \triangleq (82\mu m \times 82\mu m))$. The bottom row of Fig. 2 shows the tracks for a 100×100 section of a video (at frames: 10, 30, 45 and 70). The top row shows the tracks for the same (full) video. It is very difficult to obtain tracks for all vesicles manually, however upon inspection most vesicles seem to be tracked accurately. To demonstrate the robustness of our algorithm we do a comparison with [10], where the RMSE between tracks obtained using our method and u-track was 4.19.

5. CONCLUSION

Here we have presented an approach to tracking vesicles in fluorescence light microscopy time-lapse images. Our method uses a RJMCMC approach where two sets of dimensional altering moves are used: birth and death, and merging and splitting. We incorporated a penalization scheme to prevent trackers from converging on the same object. A similar penalization scheme is also used to distinguish between birth/splitting and death/merging. The proposed method is evaluated on a set of synthetic images, with varying SNR's. Our approach gives competitive results compared to other state-of-the-art methods. Results are also compared against u-track on fluorescence images of vesicles, however u-track contained many spurious detections. Our automated approach will enable biologists to analyze larger amounts of data and identify important events with greater accuracy.

REFERENCES

- [1] B. Alberts, B. Johnson, J. Lewis, M. Raff, K. Roberts, and P. Walter, "Visualizing cells," *Mol. Biol. Cell*, 2008.
- [2] L. Liang, H. Shen, P. De Camilli, and J.S. Duncan, "A novel multiple hypothesis based particle tracking method for clathrin mediated endocytosis analysis using fluorescence microscopy," *IEEE Trans. Image Process.*, vol. 23, no. 4, pp. 1844–1857, Apr. 2014.
- [3] W.J. Godinez, M. Lampe, S. Wörz, B. Müller, R. Eils, and K. Rohr, "Deterministic and probabilistic approaches for tracking virus particles in time-lapse fluorescence microscopy image sequences," *Med. Image Anal.*, vol. 13, no. 2, pp. 325–342, 2009.
- [4] A. Carmia, F. Septier, and S.J. Godsilla, "The Gaussian mixture MCMC particle algorithm for dynamic cluster tracking," *Automatica*, vol. 48, no. 10, pp. 2454–2467, 2012.
- [5] L. Mihaylova, A.Y. Carmi, F. Septier, A. Gning, S.K. Pang, and S. Godsill, "Overview of Bayesian sequential Monte Carlo methods for group and extended object tracking," *Digit. Signal Process.*, vol. 25, no. 0, pp. 1–16, 2014.
- [6] Z. Khan, T. Balch, and F. Dellaert, "MCMC-based particle filtering for tracking a variable number of interacting targets," *IEEE Trans. Pattern Anal. Mach. Intell.*, vol. 27, no. 11, pp. 1805–1819, Nov. 2005.
- [7] W. K. Hastings, "Monte Carlo sampling methods using Markov chains and their applications," *Biometrika*, vol. 57, no. 1, pp. 97–109, 1970.
- [8] N. Chenouard and et al., "Objective comparison of particle tracking methods," *Nat. Methods*, vol. 11, no. 2, pp. 281–289, Mar. 2014.
- [9] P.J. Green, "Reversible jump Markov chain Monte Carlo computation and Bayesian model determination," *Biometrika*, vol. 82, pp. 711–732, 1995.
- [10] K. Jaqaman, D. Loerke, M. Mettlen, H. Kuwata, S. Grinstein, S. L. Schmid, and G. Danuser, "Robust single-particle tracking in live-cell time-lapse sequences," *Nat. Methods*, vol. 5, no. 8, pp. 695–702, Aug. 2008.